Reconstruction of Man-Made Objects from High Resolution SAR Images[1]

Regine Bolter
Computer Graphics and Vision
Graz University of Technology
A-8010 Graz, Inffeldgasse 16/2
+43 316 873 5024
bolter@icg.tu-graz.ac.at

Abstract—In this paper we present our concept to reconstruct the structure of building ensembles from high resolution interferometric and slant range SAR data. To fully automate the building reconstruction procedure we want to use a phenomenological approach, using layover and shadow boundaries together with edge information and intelligent combinations of measurements from all IFSAR data sources available. For a better understanding of the geometry and phenomenology of the SAR imaging process of buildings we created a work environment with a simulator to produce magnitude slant range SAR images. As a first attempt to this phenomenology based approach we demonstrate the reconstruction of a single building. Starting from simulated test data we developed automated reconstruction algorithms from slant range shadow boundaries. These algorithms were then applied to original SAR data from the MOUT testsite. Compared to interferometric height measurements the results of our approach were quite promising.

TABLE OF CONTENTS

1. INTRODUCTION

SAR imagery has begun to get consideration as a source for three-dimensional building models. Airborne sensors deliver high resolutions at pixel sizes of 30 cm to 10 cm and single pass interferometry supports the geometric reconstruction of various small man-made objects. Interferometrically derived digital elevation models are usually less detailed than the basic magnitude images, and suffer from effects of image blur, speckle, layover, and shadows. However, measurements of building dimensions are feasible in slant range magnitude SAR images employing shadow boundaries, layover areas and edge information. We denote these as «phenomenological» features.

Our work aims at the full automation of building reconstruction using a phenomenological approach with slant range SAR images and employing interferometric observations as a guide. In this paper we present our overall strategy and first fully automated reconstructions of building shapes.

Previous demonstrations of such measurements were based on manual work, some limited automated methods for building detection and localization from IFSAR data can be found. In [1] fusion of IFSAR and multispectral image data results in boundary boxes of buildings. [2] describes an automated region growing approach to localize buildings starting from the shadows they cast. The reconstruction of building shapes of urban tower blocks from IFSAR data applying a range segmentation algorithm is presented in [3]. Another approach to enhance the quality of IFSAR imagery is described in [4].

2. CONCEPT

Airborne single pass interferometric SAR sensors deliver a variety of data products. Starting from slant range magnitude SAR images an interferometric height map and the corresponding correlation map is computed. This interferometric height map is used for a ground range transformation of the magnitude images. In contrast to most of the previous demonstrations of building reconstruction, like in [1],[2],[3],[4], which are usually performed on a single data source of an IFSAR dataset, we want to employ the best source for each single measurement and combine the results in an intelligent way.

For example the interferometrically derived height map is usually less detailed than the basic slant range magnitude SAR image and suffers from image blur effects. In slant range SAR images, buildings are easy to discern and characterized due to phenomenological features, e.g. layover areas, shadow boundaries and edge information. Starting from simulated images we want to exploit these features for building reconstruction and combine the measurements with information extracted from the interferometric data.

[1] 0-7803-5846-5/00/$10.00 © 2000 IEEE

As a first attempt to this phenomenology based approach a single building is reconstructed from the shadows it casts in slant range magnitude SAR images.

3. SAR IMAGE SIMULATION

To better understand the geometry of SAR images of buildings and the interference of buildings that exist adjacent to one another, we created a work environment with a simulator to produce magnitude images and interferometric data.

Simulating SAR images consists of two main tasks: synthesizing gray tones and incorporating imaging radar geometry. Various types of simulators exist. According to the classification in [5] we applied an incoherent image simulation method, simulating the effects of local incidence angle geometry using a DEM and ray optics. A good example for this technique is presented in [6]. Because we want to reconstruct the geometry of the building our main concern is directed towards an exact geometric simulation of the SAR imagery. Therefore in contrast to the so-called object-space approach applied in [6] to simulate a ground range SAR image, we used the so-called image-space approach to simulate a slant range SAR image. Although this approach is rather complex and time consuming, the entire regular raster of the simulated image is created with simultaneous detection of layover pixels. The extension to calculate shadow pixels and simulate interferometric data is straightforward.

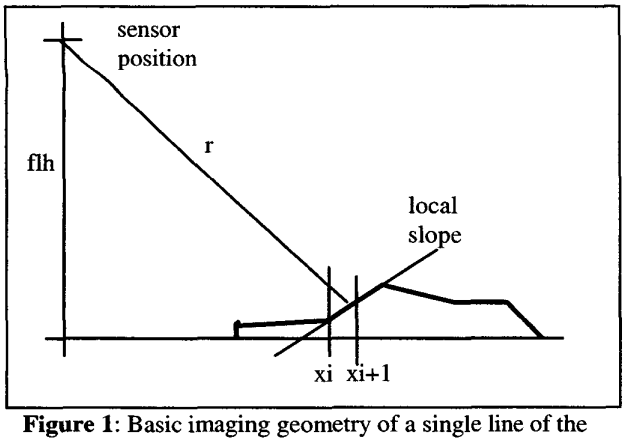

Figure 1: Basic imaging geometry of a single line of the SAR image simulator.

Because we want to study the SAR imaging geometry of rather small structures like single buildings or groups of buildings, we start from a high resolution digital elevation model (DEM) in cartesian coordinates and a quite simple straight flight path perpendicular to the DEM. This flight path is defined by the height flh above the DEM terrain and the look angle α to the starting point of the DEM. The SAR images are calculated line by line, the basic imaging geometry of such a single line can be seen from Figure 1. Each line in the SAR image is calculated as follows. For each range bin of the resulting SAR image the whole DEM line profile is checked from left to right. The range line of length r (corresponding to the range bin in the final image) is intersected with the straight line connecting two adjacent points xi and xi+1 in the DEM line profile. A target is found if the intersection lies within the range xi and xi +1. So for each xi in the line the quadratic equation

$$r^2 = (flh - dem(x,y))^2 + x^2$$

is checked for solutions in the interval [xi, xi+1]. Where r denotes the actual length of the range, flh is the sensor flight height, dem(x,y) is the actual DEM height and x is the distance from the sensor foot point to the position in the DEM. If a solution for this equation is found, the corresponding backscatter value has to be calculated The local incidence angle Θ is defined from the look angle α and the local terrain angle:

$$\Theta = \left| \arcsin(x/r) - \arctan(\Delta dem/\Delta x) \right|$$

The backscatter value is then calculated from a simple cosine model, which originally derives from modelling a Lambertian surface:

$$backscatter = \cos\Theta/\sin\Theta + \cos^3\Theta$$

This simple radiometric model for the SAR sensor is sufficient for our case, because we concentrate on geometric properties of the simulated images. Further examples of often used analytical backscatter models are the formulae developed by Hagfors [7] and Muhleman [8] in the context of astronomical applications.

In the case of layover, when more than one point of the DEM is imaged by the sensor at the same time, the backscatter values in the corresponding range bin sum up. Therefore layover is simulated automatically by this approach.

For the proper consideration of shadow, the maximum look angle and the x-position of the DEM point imaged under this look angle is stored. The backscatter value of a new point is only added to the backscatter sum of the corresponding range cell, if the x-position is lower than the stored x-position of the point imaged under the maximum look angle.

Figure 2 shows a shaded view of a simple building DEM. This DEM was input to our simulator. The DEM was simulated from the left and from the backside. The results can be seen from Figure 3.

For comparison, original SAR images of a similar building imaged from two perpendicular flight paths can be seen from Figure 8 and 9. The most significant difference between original and simulated images results from the speckle effect, not modeled by the simulator thus far.

Two different approaches to incorporate speckle into our simulation system are feasible. An attempt to incorporate speckle after the simulation process into noise-free simulated SAR images is described in [9]. Another possibility would be to modify the DEM points with proper modeled noise and simulate the images from this corrupted DEM.

However, the phenomenological features correspond between original and simulated images, layover and shadow areas are clearly discernible from other features in the real and simulated images.

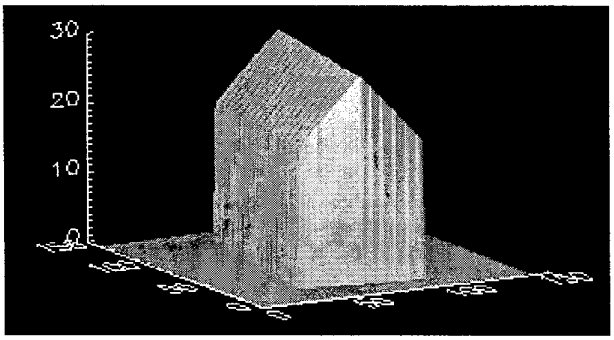

Figure 2: Shaded view of a simple building model.

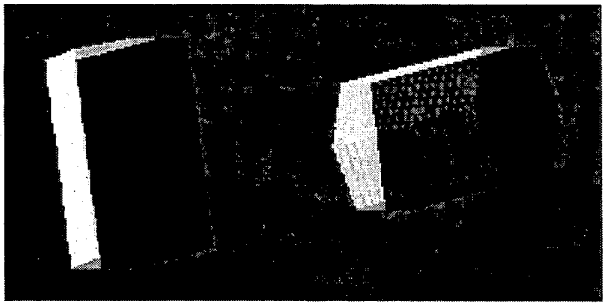

Figure 3: Simulated SAR images of the DEM in Figure 2. The left image was simulated from the left of the building model, the right image was imaged from the back side of the building model as seen from the shaded view. White pixels correspond to layover, black pixels are shadow areas and the different greyvalues correspond to different local incidence angles of the underlying surfaces.

4. Reconstruction from Simulated Images

From the position and length of the shadows in a single slant range image, one can calculate the position and height of all walls facing away from the sensor and reconstruct the underlying geometry of the building. This represents one or two walls in the case of a rectangular building. Figure 4 shows the geometry of this reconstruction.

The relative height Δh and position Δx can be calculated from the shadow length in slant range S_{sl} and the corresponding local look angle α from the equations:

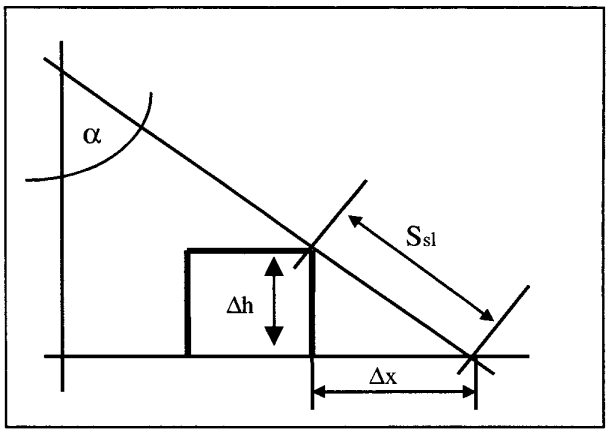

Figure 4: Slant range shadow reconstruction geometry.

$$\Delta h = S_{sl} * \cos \alpha$$

$$\Delta x = S_{sl} * \sin \alpha$$

Ambiguities exist in the definition of a wall due to layover and shadow effects in the images, for example if the roof slope exceeds the SAR look angle or if the surrounding terrain is not flat.

The next step was to segment the shadow areas from the simulated SAR images. In the case of the noise free simulated images this task is quite simple, the backscatter values in shadow areas are zero and therefore different to all other areas, a single value threshold was sufficient. The start and beginning of all shadow areas were marked in each image line and the shadow length in slant range direction (S_{sl}) and the local look angle α were inferred. Therefrom the height and position offsets can be calculated according to the equations above. The footprints resulting from the position offsets can be seen in Figure 5.

Figure 6 shows a shaded view of the resulting walls. Note that in both Figures 5 and 6 at both ends of these walls some errors are visible This is due to the fact, that the shadows in these areas are overlaid by layover areas from the

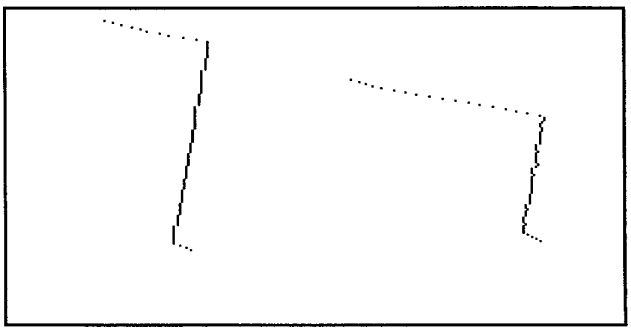

Figure 5: Resulting footprints of the building reconstruction from simulated slant range shadows.

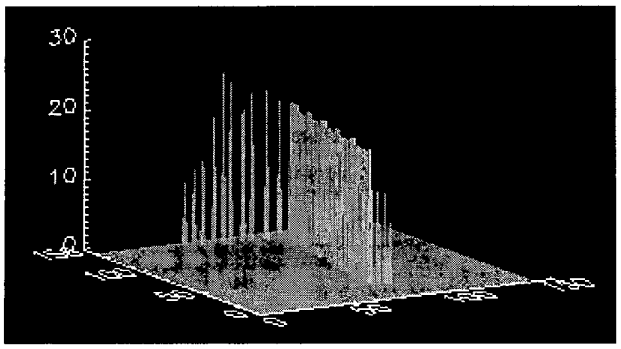

Figure 6: Shaded view of the resulting walls from the slant range shadows from the simulated SAR image on the left of Figure 3.

opposite walls. Therefore from a single image only parts of two walls can be recovered. To reconstruct a whole building only from shadows more than one view is necessary. We simulated four images using a rectangular flight path over the DEM and fused the resulting walls accordingly.

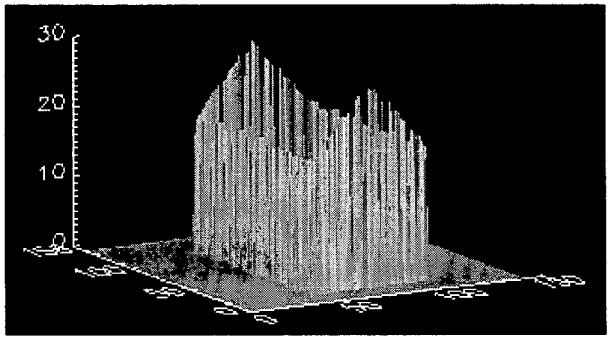

Figure 7: Fusion of reconstructed walls from four rectangular simulated SAR images.

Figure 7 shows the result of this combination process. First in the reconstruction from the single images, the wrong points at both ends of the footprints were deleted, the results were rotated according to the simulated imaging geometry of the four directions and then the results of all four directions were integrated in a single image. If for a pixel in the resulting image more than one height value from the four single images exist, the biggest value was chosen in this case. This quite simple fusion scheme worked well for this ideal simulated case, as can be seen from Figure 7.

Our next step was to apply the procedure developed for the simulated SAR images to original slant range SAR images. This is described in the next section.

5. Reconstruction from original Images

Original image test data are used from the MOUT testsite (USA) imaged from four cardinal azimuth directions with a Sandia Spotlight sensor. The slant range images have a resolution of 0.3 m.

To apply the algorithms developed in the last section to original slant range SAR images, first the shadow areas have to be segmented. In our test dataset the radiometric resolution in the slant range images is quite poor, only seven different greylevels occur. A single threshold segmentation, as was used for the simulated SAR images is not sufficient in this case, speckle statistics have to be taken into account. Speckle is often modeled as a multiplicative random noise which follows a Rayleigh probability distribution [10]. Due to this multiplicative nature shadow areas casted by the buildings are quite dark homogenous regions, however many other dark pixels exist in the image. Therefore first a 3x3 lowpass filter was applied to the images. This procedure delivered new greyvalues. The images were binarized using a greylevel threshold of 3. Region labeling was applied to the resulting binary image and small regions with less than 50 pixels were deleted. Because the boundaries of the shadow areas are the most important part for our reconstruction the resulting labeled regions were morphologically dilated three times and the resulting regions were multiplied with the original unfiltered images. For our test images with a quite poor radiometric resolution this rather simple segmentation scheme was sufficient, otherwise more sophisticated texture models should have been taken into account. The segmentation procedure was applied to all four scenes of our testdata. The results for a single house from two different directions can be seen from the right images in Figure 8 and 9.

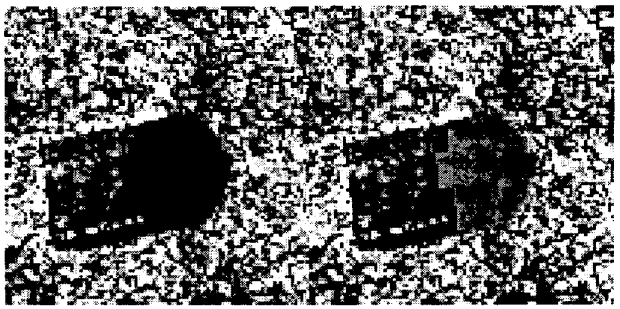

Figure 8: Single house from real SAR slant range image on the left and overlaid segmented shadow on the right-hand side.

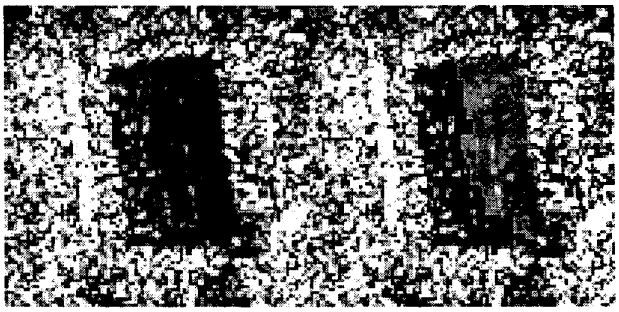

Figure 9: The same house as in Figure 8 seen from above. On the left the section from the original slant range image, and overlaid segmented shadow on the right.

The next step was to calculate the relative height and position of the walls casting the shadow, from the shadow length in slant range direction. The resulting footprints can be seen from Figure 10.

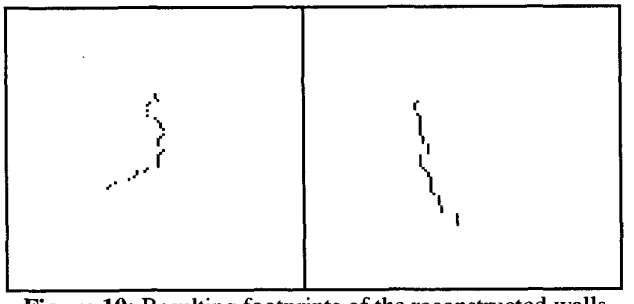

Figure 10: Resulting footprints of the reconstructed walls from the segmented shadows in Figure 8 (left) and Figure 9 (right).

In contrast to the simulated images, due to speckle effects and segmentation problems, the resulting building boundaries are quite disturbed and not so well defined as in the real image. The same problems at both ends of the footprints exist. Figure 11 shows the combination of the footprints from all four cardinal directions.

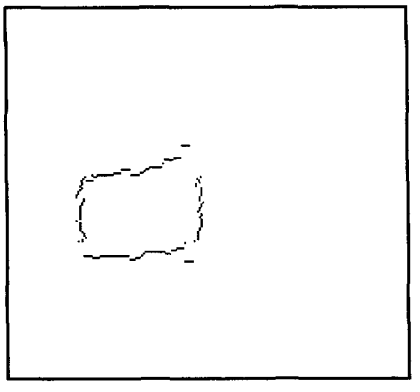

Figure 11: Combination of the reconstructed building wall footprints from real slant range SAR images from four cardinal directions.

The same fusion strategy as used for the simulated images was applied to the reconstruction results of the original images. If more than one height value existed for a single point in the fused image, the maximum value was chosen at that position. A shaded view of the result can be seen from Figure 12. The overall structure and dimensions of the building can be recognized from his view.

This whole slant range shadow reconstruction procedure results only in the walls of the building. To interpolate the building shape in between these walls, first points along the gable of the building are needed. In this case this was done manually, the two highest points of the building's walls were connected by a straight line. These points together with the other fused wall points were input into the standard triangulation and interpolation procedure of IDL [11]. The result can be seen from Figure 13.

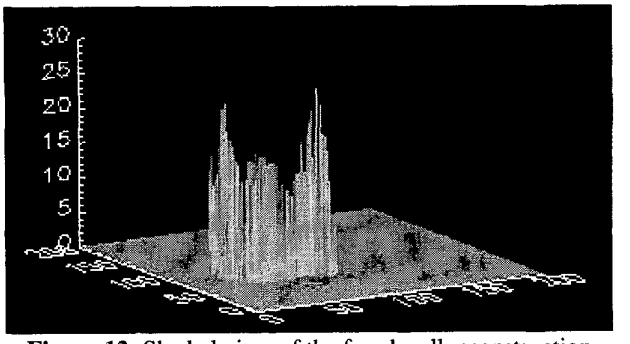

Figure 12: Shaded view of the fused wall reconstruction from four slant range SAR images from four cardinal directions.

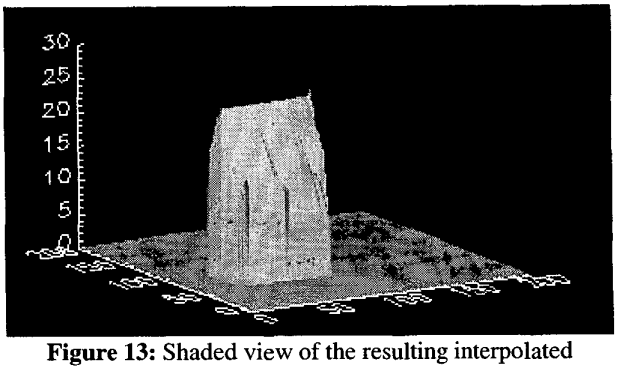

Figure 13: Shaded view of the resulting interpolated reconstructed building.

6. Comparison of Results

As was stated previously, the test data set consists of interferometric and corresponding slant range SAR data. For comparison, the interferometric height map at the same position as the reconstructed building is shown in Figure 14. This interferometric height map was fused from the interferometric measurements from the four imaging directions. At each position, the height value from the four images, with the maximum corresponding correlation value was chosen.

Comparing the results in Figure 13 and 14 with the optical images which also exist for the MOUT testsite, shows that the building structure is much better covered by the reconstruction from the slant range SAR images. In the interferometric height map, the building is difficult to distinguish from the surrounding terrain, the structure is not that obvious as from the reconstructed slant range shadows.

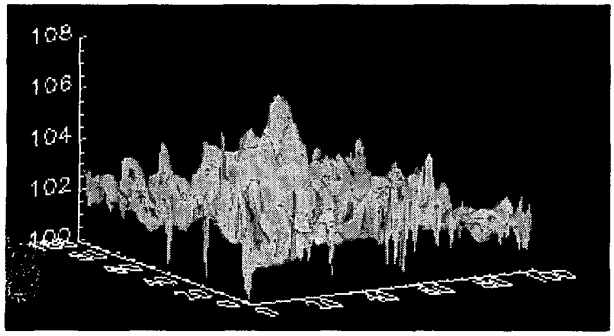

Figure 14: Shaded view of the section of the fused interferometric height map corresponding to the building in Figure 13.

Quantitative measurements of the reconstruction from slant range SAR images were not possible, because exact flight parameters were not available for this test dataset.

7. Conclusion

We have presented our concept for building reconstruction from high resolution interferometric and slant range SAR datasets. To better understand the geometry of SAR images of buildings and interference of buildings that exist adjacent to one another, we created a work environment with a simulator to produce magnitude images. A simple building model was simulated from various sensor positions. We demonstrated the effectiveness of an automated reconstruction strategy using such simulated noise free shadow boundaries. The same procedure was then applied to a similar building imaged by Sandia's Spotlight sensor. In comparison to the information delivered by the interferometric height map, which was also available for this testsite, the building structure recovered from slant range shadow boundaries was significantly better. Quantitative measurements were not possible because no exact flight parameters were available for the test data.

The extension of the presented algorithm to building ensembles were shadow boundaries interfere with other buildings remains a question for further work.

References

[1] R. Xiao, C. Lesher and B. Wilson, Building Detection and Localization Using a Fusion of Interferometric Synthetic Aperture Radar and Multispectral image, *ARPA Image Understanding Workshop,* 583-588,1998.

[2] K. Hoepfner, A. Hanson and E. Riseman, Recovery of Building Structure from SAR and IFSAR Images, *ARPA Image Understanding Workshop,* 559-563, 1998.

[3] P. Gamba and B. Houshmand, Three Dimensional Urban Characterization by IFSAR Measurements, *Proceedings of IGARSS 1999.*

[4] G.R. Burkhart, Z. Bergen and R. Carande, Elevation Correction and Building Extraction from Interferometric SAR Imagery, *Proceedings of IGARSS 1996,* 659-661.

[5] F. Leberl, *Radargrammetry,* Artech House, 1990.

[6] M. Gelautz, H. Frick, J. Raggam, J. Burgstaller and F. Leberl, SAR image simulation and analysis of alpine terrain, *ISPRS Journal of Photogrammetry & Remote Sensing* 53 (1998) 17-38.

[7] T. Hagfors, Backscattering from an undulating surface with applications to radar returns from the Moon. *Journal of Geophysical Research,* 69(18),3779-3784,1964.

[8] D. Muhleman, Radar scattering from Venus and the Moon, *Astronomical Journal,* 24,34-41,1964.

[9] R. Bolter, M. Gelautz, F. Leberl. SAR Speckle Simulation, *Int. Arch. Photogramm. Remote Sensing* 31(B2),20-25.

[10] J.W. Goodman, Statistical Properties of Laser Speckle Patterns. In *Laser Speckle and Related Phenomena,* J.C. Dainty, ed., Springer Verlag, Berlin, 1975.

[11] IDL (Interactive Data Language), User Manual, Version 3.6.1.a, Research Systems Inc. Boulder CO, 1994.

Regine Bolter *was born in Bregenz, Austria in 1971. In 1990 she graduated from the Höhere Technische Lehranstalt für Elektronik und Nachrichtentechnik in Rankweil with distinction. She started to study Telematik at the Graz University of Technology and received the Dipl.-Ing. Degree with distinction in 1997. Since 1995 she is a member of the Remote Sensing group at the Computer Graphics and Vision Institute at Graz University of Technology. Currently she is working towards the Dr.techn. degree. Her main fields of research are SAR image analysis and simulation.*